Impact of plasma shaping on electromagnetic microinstabilities

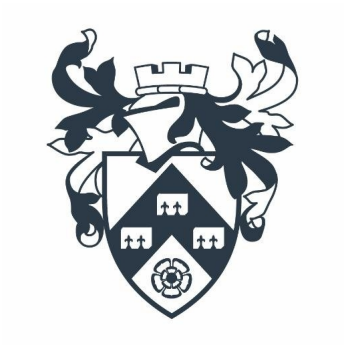

UNIVERSITY of York

This dissertation is being submitted for the partial completion of the MSc fusion course.

Alexei Kosykhin supervised by Dr David Dickinson

September 2017

Abstract

An investigation was performed by a computer simulation how plasma shaping effects micro instabilities in a tokamak. The investigation was conducted by using a linear gyrokinetic code GS2 with circle shifted MILLER geometry[1]. The code consistence and correctness were verified by a number of convergence tests showing positive results regarding all its main input parameters. In addition, the scan of the plasma growth rate and frequency against plasma performance, β, has a good agreement with the published results[2]. The computer simulations showed the presence of the Ion the Temperature Gradient (ITG) mode at low β, but at β > 1% the ITG mode disappears and the the Kinetic Balloning Mode (KBM) becomes dominant. The studying of the KBM was the priority because of its important role in the EPED model[3]. According to the the EPED model the height and the width of the tokamak pedestal is determined by two main physical constraints: the ELMs modes and the KBM. The higher and wider the pedestal, the better tokamak performance. The GS2 code was slightly enhanced to take into account the Shafranov shift and demonstrate that the shift suppresses the KBM. It was found that a plasma behaves differently depending on β. At the high β, at elongation of the torus cross section, κ > 1.5 the KBM disappears and the plasma growth rate becomes very low. The plasma growth rate, γ, is very sensitive to elongation, κ, but has a weak dependence on triangularity, δ, and other geometry parameters. The results can be explained by theory of “bad/good” curvatures, analysis of the gyrokinetics equation. The results can be understood in terms of “s-α” model[2].

1. Introduction

As our civilization has entered the technological era, the amount of energy usage becomes the essential criteria for its successful development. According to the Kardashev scale[4], the more amount of energy a civilization uses the higher its level of technological advancement is. Currently our civilization can be classified only as a Type Zero or a sub-global civilization, which controls only its own planet. Hopefully our next level will be a Type One civilization, which probably will employ a large scale of fusion power.

Nowadays we produce the most energy from fossil fuel such as oil and natural gas. However the fossil fuels are expensive and and their deposits are limited. The amount of energy produced from the fossil fuels can not meet our energy demand in full - many nations still have a very modest access to energy sources. Furthermore, the production of energy from fossil fuels pollutes the environment, produces green house gases such as carbon dioxide, which causes global warming.

1.1 Fusion

From this point we need to find a better, cheaper and cleaner source of energy. Along with solar and other renewable sources of energy, fusion can be a good option. Fusion energy is a clean, inherently safe and promises an unlimited source of energy. Nuclear fusion is based on the phenomena of merging two light nuclei into a heavier nucleus and releasing an ample amount of energy. The most promising fusion reaction is D + T = He + n + 17.3 MeV, where D is a hydrogen isotope, Deuterium, T is a hydrogen isotope, Tritium, He is Helium, n is neutron, 17.3 MeV is the amount of energy realised. Reserves of Deuterium are huge while Tritium does not occur in nature, but it can be produced from Lithium. Reserves of Lithium are also huge. Deposits of fuel for fusion are enormous and will be sufficient for a long time.

There are two main ways to achieve fusion: Magnetically Confinement Fusion (MCF) and Internal Confinement Fusion (ICF). There are two types of MCF devices: tokamaks and stellarators. In my research I will consider only tokamaks. A tokamak is a device which confines a plasma in a shape of an axially symmetric torus. Tokamaks can be various sizes and shapes and have different performances.

It has been observed that plasma physics and the tokamak performance depend on its size and shape [5]. It was suggested that the curvature of magnetic flux surfaces plays the key role in this process. But the curvature of the magnetic flux surfaces depends on the plasma parameters and tokamak shape, the elongation and the triangularity of the cross section of its torus. However plasma of physics of this process is not fully understood and we need further study of this problem.

Although physical experiments is a very proper and reliable way for studying plasma physics, it remains very expensive and not always affordable. An alternative way to study plasma is by computer simulations, which is many thousand times cheaper but very effective.

1.2 Introduction to Gyrokinetics

In computer simulations we use gyrokinetic code, which based on theoretical framework for studying plasma behaviour. A starting point of gyrokinetics is the Vlasov equation, which describes a system of charged particles in 6 phase space: 3 dimensions for the space coordinate and 3 dimensions for the velocity coordinate. The Vlasov equation has the form:

$$\frac{\partial f}{\partial t}+\boldsymbol{v}\cdot\frac{\partial f}{\partial \boldsymbol{x}}+\frac{q}{m}\left(\boldsymbol{E}+\boldsymbol{v}\times\boldsymbol{B}\right)\cdot\frac{\partial f}{\partial \boldsymbol{v}}=C(f) \qquad (1)$$

$\frac{\partial f}{\partial t}$ is changing of the distribution function in time,

$\boldsymbol{x}$ is 3 dimensional coordinate, $\boldsymbol{v}$ is 3 dimensional velocity,

$\frac{q}{m}\left(\boldsymbol{E}+\boldsymbol{v}\times\boldsymbol{B}\right)$ is the Lorentz force,

$\boldsymbol{E}$ is the electric field,

$\boldsymbol{B}$ is the magnetic field,

$C(f)$ is a collisional operator.

The full 6 dimensional Vlasov equation describes the movement of the system of so many particles that it can not be solved even by modern supercomputers. To solve the Vlasov equation we need somehow to simplify it. Gyrokinetic theory offers a number of methods and techniques to simplify the Vlasov equation and derive a gyrokinetic equation, which can be solved numerically.

The first step of simplifying of the equation is the expansion and linearisation of the Vlasov equation by splitting the distribution function into main and a perturbed parts: $f=F_0+f_s$
The next step is making the following assumptions, which will simplify the equation further:

- perturbations are much smaller than the distribution function,
- particles move only along field lines,
- perturbations vary much quicker than the equilibrium,

These assumptions give us such a called gyrokinetic ordering[6]:

$$\frac{\Omega}{\omega_c}\sim\frac{\rho}{L}\sim\frac{k_{\parallel}}{k_{\perp}}\sim\frac{L_{\perp}}{L_{\parallel}}\sim\delta\ll 1 \qquad (2) \qquad ,$$

Ω is the global frequency, ω_c is plasma frequency, ρ is the Larmour radius,
L, $L_{\parallel}$, $L_{\perp}$ are some characteristics of length scale, δ is a small number.

However the major achievement of gyrokinetic theory is simplifying the Vlasov equation by averaging the gyro-velosity. According to the single particle kinetics, a single charged particle gyrates along a magnetic field line and its trajectory looks like loops. By averaging over these gyro-motions and considering these loops as single moving dots, gyrokinetics reduces the 6 dimensional the Vlasov equation into a 5 dimensional.

Looking back at history the following milestones in developing gyrokinetics took place:

- The Vlasov equation was published in 1937. It had an unusual form for us and it was written for three species – ions, electrons and neutrals. It was impossible to solve the equation because computers did not exist then and the equation had only analytical implications. It took a few decades to develop modern gyrokinetics from of the Vlasov equation:

-The linear theory was introduced by J. B. Taylor and R. J. Hastie, Rutherford and Frieman in 1968,

-Nonlinear theory by Frieman and Chen in 1972,

-Computer first simulations by W. W. Lee by 1983,

-Hamiltonian formulation which ensures conservation of energy by R. C. Little John in 1979,

-Modern gyrokinetics uses advanced mathematics of differential anemometry field theory.

Success of gyrokinetics depends on computer power, the more computer power, the easer to solve it. Gyromagnetics looks a very promising field of research because computer power is still increasing, and gyrokinetic simulations have a good agreement with experiments. The modern gyrokinetic equation has the form:

$$\frac{\partial \bar{f}_1}{\partial t}+\boldsymbol{V}_0\cdot\frac{\partial \bar{f}_1}{\partial \boldsymbol{X}}+C\bar{f}_1=i\omega e\left[J_0(k_\perp\rho)\left(\Phi_A-\frac{u}{c}A_{\parallel A}\right)+\frac{s}{ck_\perp}J_1(k_\perp\rho)B_{\parallel A}\right]\cdot$$
$$\cdot\left[\frac{\partial f_0}{\partial U}+\frac{c}{eB_0}\boldsymbol{k}\times\boldsymbol{b}\cdot\nabla f_0\right] \qquad (3)$$

The main its terms and parameters are described bellow:

$\frac{\partial \bar{f}_1}{\partial t}$ is changing of the distribution function in time, $\boldsymbol{V}_0\cdot\frac{\partial \bar{f}_1}{\partial \boldsymbol{X}}$ is the conjunctive derivative,

$C\bar{f}_1$ is a collisional operator, Φ_A is the electric potential, U is the total particle energy,

u is some velocity, J_0, J_1 is the Bessel function; B_0 and $B_{\parallel A}$ are the magnetic fields, $A_{\parallel A}$ is the parallel magnetic potential; is a gyroradius, k is a wave number.

The gyrokinetic equation is only a model describing the physical process in plasma, it needs to be numerically solved. Solving the equation is still not straight forward.The following advanced numerical methods and techniques are implemented in GK2 code: Linear Implicit Algorithm, Discritisation and Parallisation, Advancing Implicity, Green's Functions, Numerical Implementation.

Varies Gyrokinetic codes exist: GS2, GKW, GENE, GYRO, GEM, GTC, XGC. Most of the gyrokinetic codes solve the equation on a single flux surface[7]. It is very important to mention that gyrokinetic codes can divided into linear and non-linear. To contrast to linear, non-liner codes take into consideration second order perturbations. Running non-linear codes takes significantly more computer power, but non-linear codes solve the problem with a much higher accuracy.

1.3 Motivation

One of the motivations of my research is studying the Kinetic Ballooning Modes (KBM), how this mode depends on tokamak parameters. According to the EPED model the KBM is a key parameter for making a shape of the tokamak pedestal, both its hight and width. The KBM is a pressure gradient driven mode, its turbulence is characterised by a short correlation time, large heat and particle transport[8]. A shape of pedestal plays a significant role in the tokamak performance and confinement because of the following reasons: a plasma at high tokamak profiles has higher pressure and temperature, pressure in the plasma core is proportional to the pedestal pressure, it is because if the whole pedestal profile starts moving up, the pressure in the centre will follow the pressure at the edge. Fusion power scales with the square of the core pressure.

To summarise this, the steeper and wider a pedestal, the better the tokamak performance and confinement[3]. This is a reason why the goal of ITER is operating in H-mode with a high pedestal.

According to the the EPED model the height and the width of the pedestal depend on two main physical constraints. The first physical constraint is defined by ELMs modes. At the edge of plasma there are a few types of ELMs modes. As it is believed, the ELMs can trigger filamentary eruptions of plasma, which eventually deteriorates the plasma confinement. The second physical constraint is caused by the KBM, which is a type of an ideal MHD ballooning mode[9].

The simplified version of EPED model is EPED1. This model suggests that the KBM constraint depends on the plasma efficiency, β, and the growth rate of the KBM scales with square root of β. The EPED model combines ELMs and KBM physics a to predict a pedestal shape. The model explains a phenomena of "the ELM cycle", it is when the KBM exceeds some stability limit and causes the ELMs to crash and the plasma pressure to drop. Knowing the stability boundary of the KBM and ELMs, the pedestal height and width can be predicted[10]. It also helps to identify stable and unstable areas of tokamak operations. This model was successfully tested in many experiments[11]. Particularly, the simplified model EPED1 has a long history and was tested on D-III-D, C-mode, JET and has a good agreement with obtained results with accuracy up to 20 %.

The ELMs are type of peeling-ballooning modes. Although the ELMs are important in the EPED model, she study of these modes will not be a part of my research. GS2, the code which I use, can solve only on a single flux surface or a field line, that is perfect for studying the KBM. However the ELMs span through many surfaces, and the ELMs can not be solved by GS2. A different type of a code, the code MHD, is required for studying the ELMs. I will focus on studying only the KBM. Although my simulations are performed at the middle flux surface, which is not very close to the edge, we are still interested in the KBM in this area because it would help to understand a role of the mode in the EPED model in general.

2. Method

In this section I outlined how my experiments/simulations were conducted. It was not physical experiments but computer simulations of the physical process. The physical process was approximated by mathematical model, then computer code solved this model by numerical methods. I suggest my result would have good agreements with experimental data.

I was conducting the simulation from my laptop, which was running on Linux OS. However the GS2 code was not in my laptop, it was installed in the machine at York University campus. Through the internet connection, using a cryptographic network protocol SSH, I had access to the machine directory, I was able to manage files, change input parameters, run simulations and get the output data back to my computer. Once I was connected to the machine directory, using "emacs" software I was able to change input parameters in "input.in" file. Here is a list of the main input parameters in "input.in" file[12].

2.1 Input and output parameters.

Table 1 contains input parameters for the first stage of simulation.

Abbreviation	*Type*	*Description, physical meaning*
beta, β	*float*	*in GS2 beta is the ratio of the reference pressure to the reference energy density. Mainly GS2 uses beta to determine the amplitude of the perturbed magnetic field.*
n_0	*integer*	*the toroidal mode number*
ntheta	*integer*	*number of grid points along equilibrium magnetic field between theta = (-π, π)*
ngauss	*integer*	*number of untapped pith-angles moving in one direction along field line*
nperiod	*integer*	*number of sets of 2π segments along equilibrium magnetic field*
negrid	*integer*	*the total number of energy grid points*

Table 2 shows the main input "MILLER" parameters with advanced geometry for second stage.

Abbreviation	*Type*	*description, physical meaning*
akapa, κ	*float*	*the flux surface elongation*
akappri, $\nabla\kappa$	*float*	*the radial gradient of flux surface elongation*
tri, δ	*float*	*the flux surface triangularity, which selects the generalised Miller analytical geometry*
tripri, $\nabla\delta$	*float*	*the radial gradient of the flux surface of triangularity, trippri =* $\frac{\partial\delta}{\partial\rho}$
rhoc	*float*	*flux surface label, or mid plane diameter, minor radius*
rmaj	*float*	*major radius of the centre of the flux surface.*

After setting initial parameters I run the code. Then after running the code for a few minutes output data was calculated and placed into OUTPUT file. This output data was distribution function f, the electric potential, Φ_A , the magnetic field, $B_{\|}$, the parallel magnetic potential, $A_{\|}$ as a functions of time. I needed to interpret this data into the data which we already know because it would help us to understand the physics. We were able to derive from this data from the electric potential, Φ_A , via time. Knowing the squared potential via time we could calculate the plasma growth rate, γ, and frequency, ω.

In my project I needed to conduct a series of scans of γ and via ω their input variables. Every single scan involves from 10 to to 40 runs depending on comprehensiveness of the scan. In the machine directory I organised sets of directories. Every directory was named according to the name of scan I performed. The directory contained approximately 50 folders every each of them had files from individual runs. Such a structure of the directories and folders helped me to manage the data properly. I did aproximately 50 scans and 1000 runs. I ceased the running code if it was running longer than 30 minutes. I recorded obtained data of growth rate and frequency in my lab book, then copied the figures into text files. By using python code I plotted the data and presented it in "png-format" images.

This method of obtaining results has some advantages and disadvantages. The main disadvantage is running the code GS2, analysing and recording results is very time consuming, it is not totally automatised and a lot of manual work is involved. The advantage is simplicity, easy to control, opportunity to stop a code when it is running too long.

My computer simulations can be divided into two stages. At first stage, when I was testing the code, I used input.in file. At second, where I studied impact of tokamak geometry on plasma physics, I used MILLER file. The two files "input.in" and "MILLER" are slightly different. The code with "input.in" file employs a simple circle model known as the "α-s" model, which allows to using of shear and pressure gradient, but does not allow to change plasma shape parameters.

2.2 Geometry

The code with "MILLER" input uses a shifted circle model, where the circle becomes a geometrically comprehensive geometric figure. This figure has the shape of the ellipse with triangular features and can be defined mathematically trough its parameters R and Z, where R and Z are functions of variable theta, θ[1].

$$R_s(\theta) = R_0 + r * \cos[\theta + \arcsin(\delta) * \sin(\theta)] \quad , \quad Z_s(\theta) = \kappa * r * \sin(\theta)$$

Where R_0 and r are the tokamak major and minor radii, κ is elongation, δ is triangularity, θ is an angle, the additional parameter helping to outline the shape. Using the equation above I draw some cartoons, showing possible geometries of the cross sections:

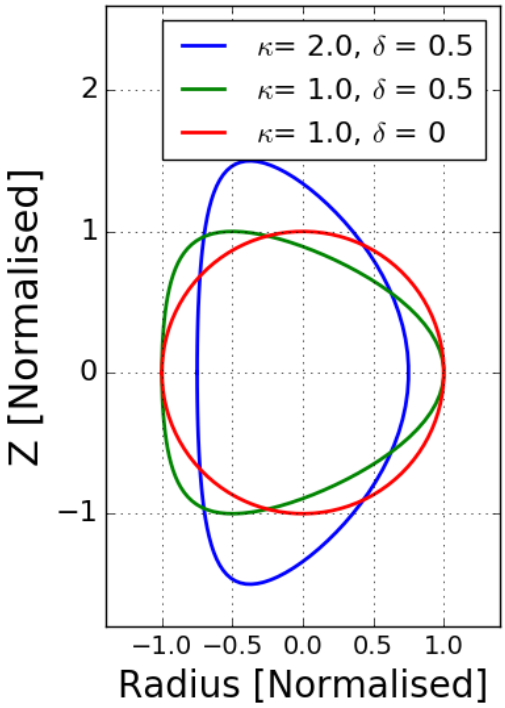

Figure 1a is a cartoon and shows altered circles with κ = 1 and δ =0; κ= 1.0 and δ = 0.5; κ =2.0 and δ = 0.5 accordingly.

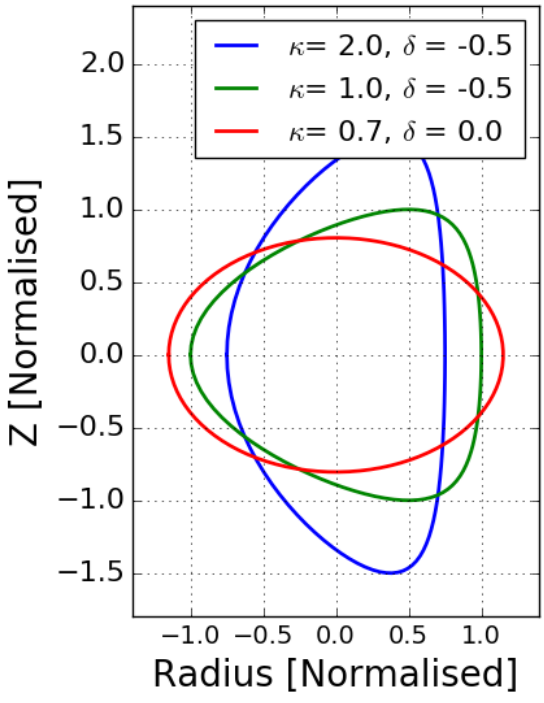

Figure 1b is a cartoon shows altered circles with κ = 0.7 and δ =0; κ =1 and δ = -0.5; κ = 2.0 and δ = - 0.5 accordingly.

The cartoons below demonstrate the elongation and triangularity derivatives, it is when the first internal flux surface is a circle but next surfaces have more elongation or triangularity features.

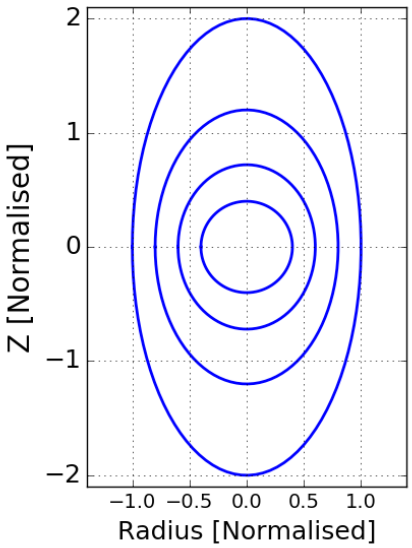

Figure 1c is a cartoon and shows a positive elongation derivative, $\nabla\kappa$

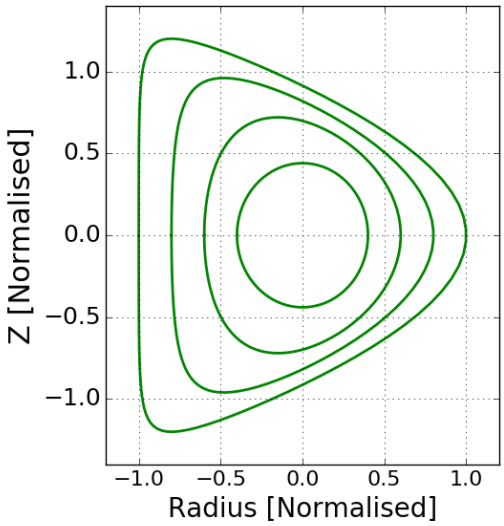

Figure 1d is a cartoon and shows a positive triangularity, $\nabla\delta$.

2.3 The Shafranov shift

According to the Shafranov shift at $\beta > 0$ the tokamak magnetic flux surfaces become shifted from the the centre to outwards. To calculate the shift I used the following formula:
shift = 2*β*(tprim + fprim)*2*(epsl)/(pk*pk). Where tprim, fprim, epsl, pk are some input parameters. Knowing the shift I was able to adjust input parameters (shift) in "input" file before running the code. The shift was recalculated for each run. For producing a report of output parameters the "ingen" file was used.

In addition, for comparison my data with journal results, I used the software programme "Engauge Digitize" and "Paint" installed in my laptop running on "Windows 7" OS. I digitised journal plots and saved the digitised data into text files, then using "python" code I plotted the data together with my results.

3. Verification of the code

To have some confidence that the computer simulation gives correct results, the validation and verification tests of the code has to be conducted. Verification is the process of assessing software correctness and numerical accuracy of output to a given mathematical model. Validation is the process of assessing the physical accuracy of a mathematical model based on computation between computational results and experimental data. But sometimes we do not know the experimental results and cannot conduct a validation test. In my research I will provide a convergence test as a part of the code verification.

By definition the convergence is the fact that two or more things become similar. Convergence in mathematics is a property, which can be exhibited by certain series and functions, of approaching limit much closely as the argument or variable of the function increases or decreases. For

example, the function y = 1/x convergences to zero as x increases. If the code converges to some limit regarding its variables, it would mean the code is correct, if not, there is some problem. There are a number of different criteria that can be used for convergent test: simple test or discretisation error evaluation, code-to-code comparison, regression testing, iterative convergence, convergence test, order-of- accuracy test, some advanced methods like Method of Nearby Problems (MNP). For example, in the simplest convergent test the verification criteria is comparing the solution to a reference solution, ideally an exact solution of the mathematical problem:

$(u - u_{ref} \to 1/N)$ or $\sum (u_n - u_{ref}) \to 0$

If a reference solution is not known, simplest converge test can not be provided. A regression testing involves the comparison of code output to output early in versions. However in some cases we do not know the exact solution of the problem. We need to compare the code with itself. We can use iterative convergence. It is comparing nearby iterates with each other.

$f_{k+1} - f_k \to 0$ or $(f_{k+1} - f_k)/f_k \to 0$ However this test can be misleading.

3.1 The code-to-code comparison

The most easiest and reliable convergence code is the code-to-code comparison, where output from one code can be compared to output from second code. However this method can be useful when the two codes employ the same mathematical models. Here I will compare my results with already results published in paper[2].

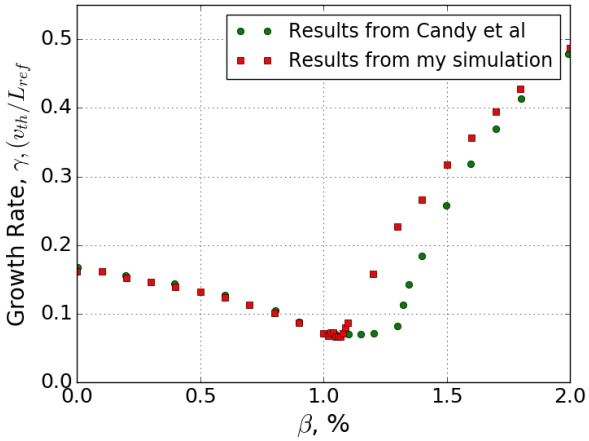

Figure 2a. Shows data of the plasma growth rates obtained from my simulation and reference paper[2]

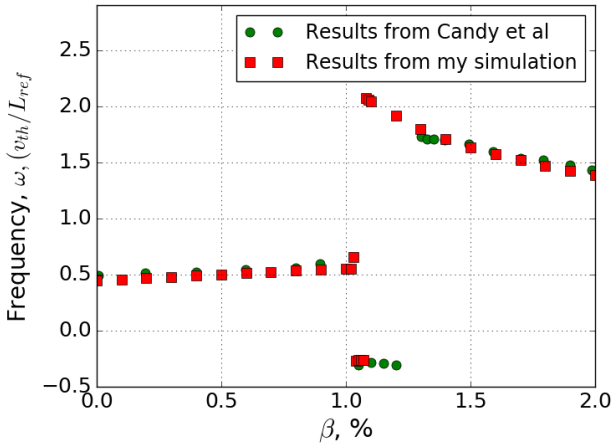

Figure 2b shows data of the plasma frequencies obtained from my simulation and reference paper [2]

As we can see from figures 2a and 2b my results look very similar to the published results. The two curves have the same shapes. Both scans show the same three modes. From β = 0 to 1.0 there is the Ion Temperature Gradient (ITG) mode. Then probably the Trapped Electron Mode (TEM) appeared. After β >1.3 both results show the Kinetic Ballooning Mode (KBM), although values of the growth rates in this β >1.3 area are slightly different. As we can see from figure 2b frequencies from the two results are absolutely the same excluding area β = 1.1 – 1.3, where the TEMs have different durations.

It is very important to note that I used a linear version of GS2, but the paper results are obtained from a non-linear code. Probably this fact explains the slight differences between two results.

3.2 The convergence tests

Here I will present results from convergent tests, showing how the plasma growth rate and frequency as functions behave when their variable, ntheta, increases.

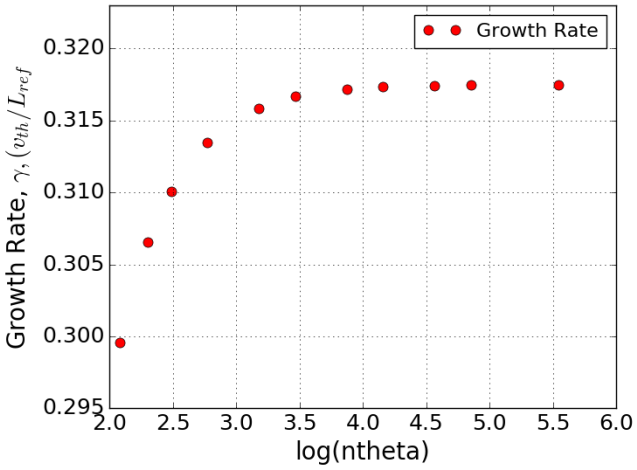

Figure 3a shows the growth rate against number of grid points, ntheta, in logarithmic scale.

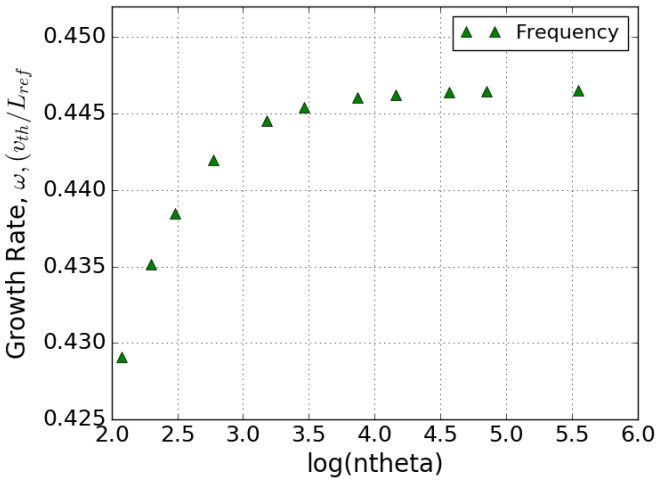

Figure 3b shows the frequency against number of grid points, ntheta, in logarithmic scale.

The integer variable ntheta is a number of grid points along equilibrium magnetic field between theta = (-π; π) and it is shown on x -axis in the logarithmic scale. For example, value of 2.0 represents ntheta = 7.39, value of 4.0 represents ntheta = 54.6.

As we can see from figure 3a the plasma growth rate smoothly approaches the limit of 0.317 as ntheta increases. I suggest that growth rate at ntheta greater than 256 will have very close or even the same value of 0.317. Figure 3b shows the plasma frequency smoothly approaches the limit of 0.453 as ntheta increases. I suggest that frequency at ntheta greater than 256 will have very close or even the same value of 0.453.

In this convergent test I did not have an opportunity to run the code at ntheta bigger than 256 because running the time would exceed 1 hour. I can conclude that the code in this particular situation satisfies the convergent criteria. In total I conducted 16 convergence tests – for the growth rate, γ, as a function via its variables - ntheta at β = 0% and 2%; ngauss at β = 0% and 2%; negrid at β = 0% and 2%; nperiod at β = 0% and 2% and for the plasma frequency, ω, via the same variables. In addition, the code is sensitive - slight changes of some input parameters causes slight changes in output. Although the code sensitivity, benchmarking and a convergence tests are only minimum criteria, it is give some confidence of the code correctness.

4. Results

4.1 The impact of the Shafranov shift on plasma behaviour

Here the results of an impact of shifted magnetic flux surfaces on a plasma behaviour are presented.

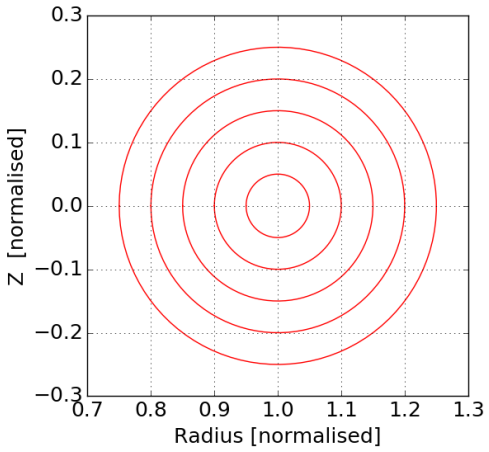

Figure 4a is a cartoon and shows geometry of the original magnetic flux surfaces.

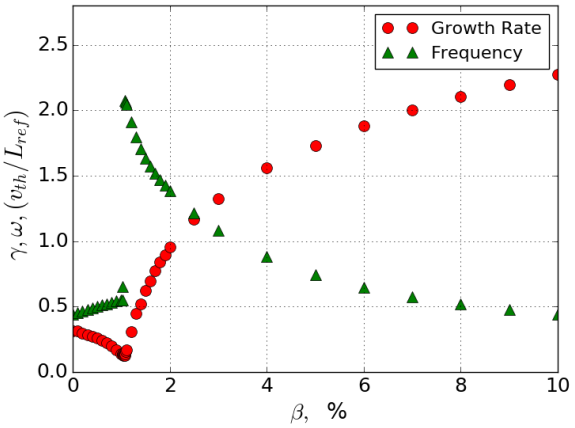

Figure 4b shows plasma growth rate and frequency at the original magnetic flux surfaces.

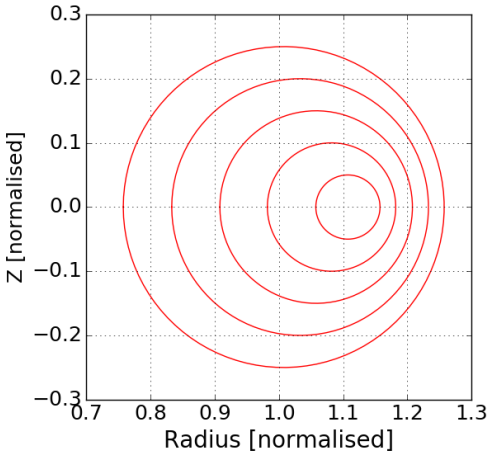

Figure 5a is a cartoon shows geometry of the shifted magnetic flux surfaces in the circular cross section of the tokamak torus.

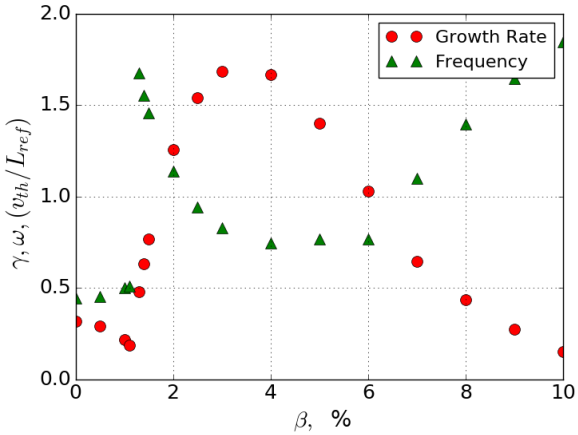

Figure 5b shows plasma growth rate and frequency at the shifted magnetic flux surfaces.

Figure 4a shows a scan of the plasma growth rate, γ, and frequency, ω, against β at the fixed magnetic flux surfaces, when a plasma does not have influence on the tokamak magnetic field. However in the real situation the magnetic flux surfaces can be altered because of a presence of a plasma. I took a scan, shown on figure 5b, of γ and ω against β at a situation when the magnetic flux surfaces are shifted backwards from the tokamak centre. The two scans show that γ and ω at the fixed and shifted flux surfaces are different - γ at the shifted magnetic flux at high β is much lesser. At both scans we see the same modes the ITG and the KBM. However at β >4% the

situation is unclear because it is difficult to identify the modes at the β >4%. Both scans were taken at the same initial parameters – the toroidal mode number n_0 = 39.

4.2 Impact of plasma shaping on plasma growth rate and frequency

In this section scans of the cross section of the tokamak torus via plasma parameters are provided.

4.2.1 The plasma growth rate and frequency against elongation, κ

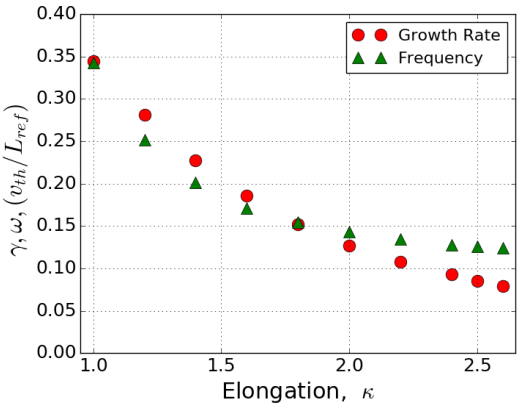

Figure 6a shows plasma growth rate and frequency as functions of κ at β = 0.5%

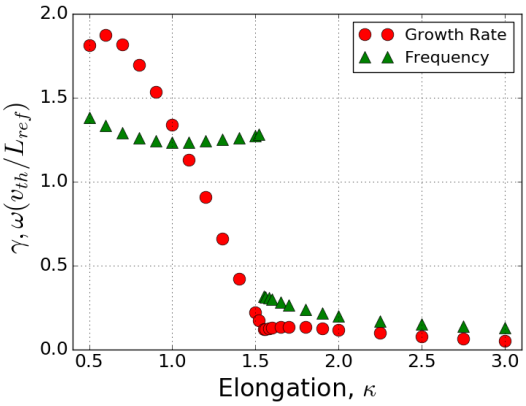

Figure 6b shows plasma growth rate and frequency as functions of κ at β = 2.0%

From these two scans we clearly see that the elongation of the cross section of tokamak torus has an obvious impact on the plasma behaviour. In general the plasma growth rate decreases with increasing elongation, κ. However, the plasma growth rates and frequencies behave absolutely differently depending on β. At the scan at β = 0.5% the γ and ω are decreasing smoothly. Their lines probably represent only the ITG. At the scan at β = 2%, the γ and ω lines have an abrupt point at β = 1.5, that indicates that the mode was changed. Actually the elongation area at β= 2% can be divided into two regions: the ITG, which is at κ<1.5 and the KBM region, which is at κ>1.5. The ITG has a weak dependence from κ, but the KBM is more sensitive to elongation, κ.

4.2.2 Growth Rate and Frequency via elongation derivative, $\nabla\kappa$

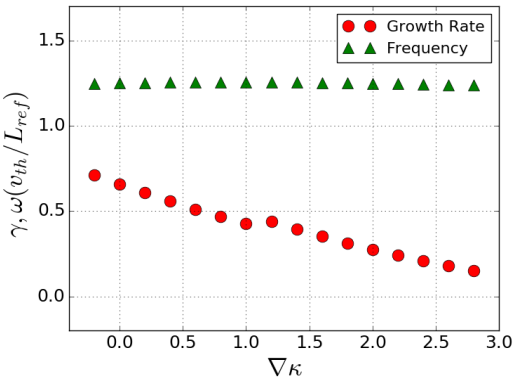

Figure 7a shows results of scan of γ and ω via $\nabla\kappa$ at κ =1.3, β =2.0%

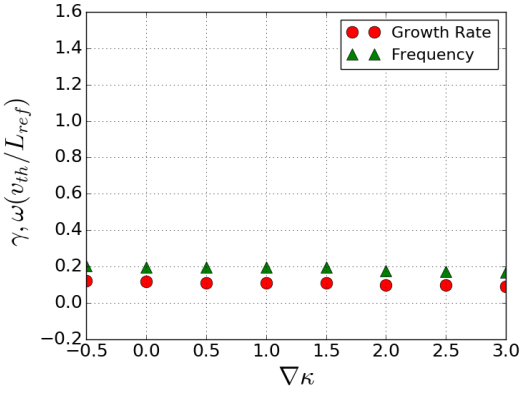

Figure 7b shows results of scan of γ ω via $\nabla\kappa$ at κ = 2.0%, β = 2% .

From figures 7a and 7b we can see that the elongation derivative, $\nabla\kappa$, has absolutely different impacts on γ and ω depending on elongation, κ. At scans 7a and 7b there are different plasma modes: at figure 7a there is the KBM, at figure 7b there is probably the ITG.

4.2.3 Impact of the triangularity on plasma growth rate and frequency

I took four scan of the growth rate, γ, and the frequency, ω, via triangularity, δ, at four different values of elongation, κ: κ = 0.6, when the cross section is "a squeezed circle"; at κ = 1, when the cross section is a circle; at κ = 1.3, when the circle is slightly elongated; and at κ = 2.0, when there is an obvious elongation. All scans were taken at the elongation derivative, $\nabla\kappa$ = 0.6, at β = 2% and n_0 = 39.

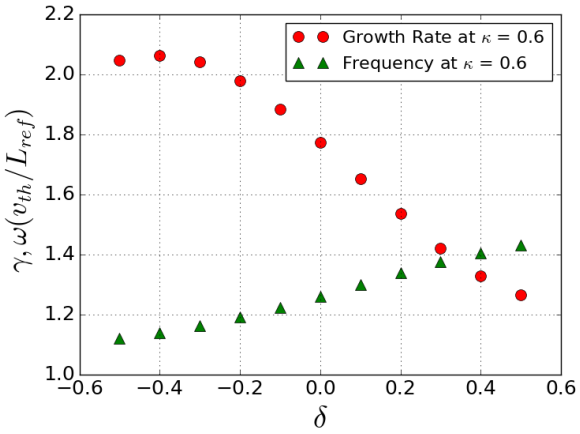

Figure 8a shows a scan of γ and ω via triangularity, δ, at κ= 0.6

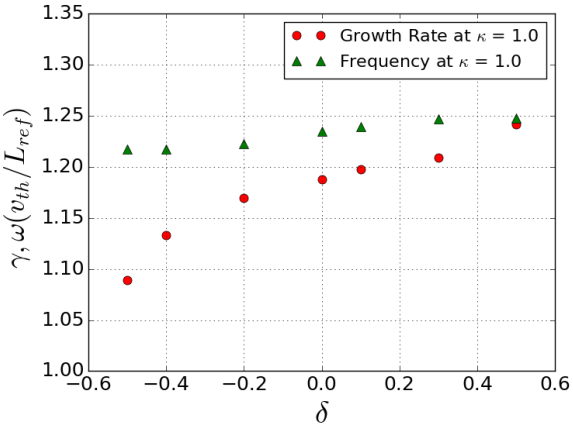

Figure 8b shows a scan of γ and ω via triangularity, δ, at κ = 1.0

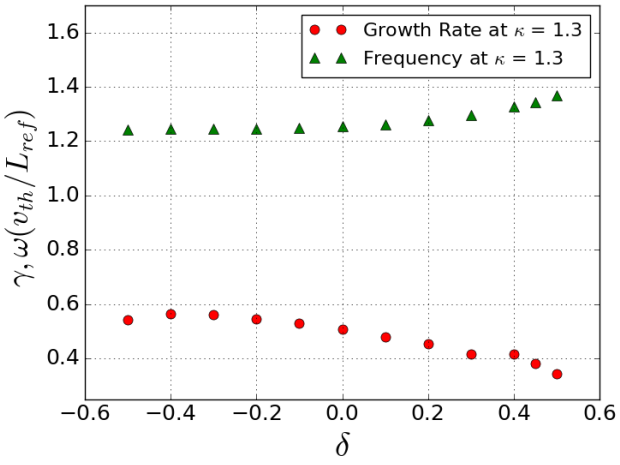

Figure 8c shows a scan of γ and ω via triangularity, δ, at κ = 1.3

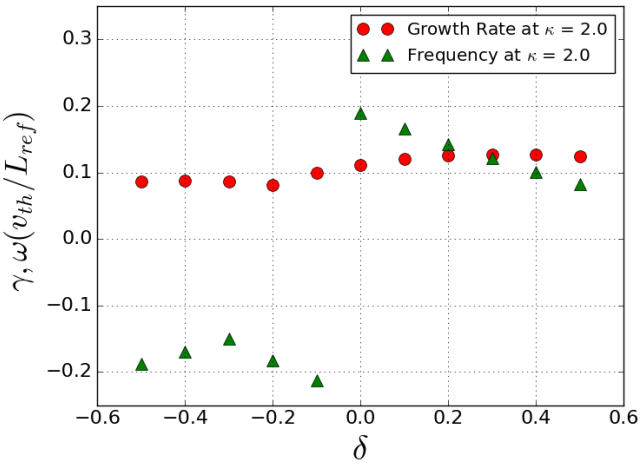

Figure 8d shows a scan of γ and ω via triangularity,δ, at κ = 2.0

These four scan clearly show that the impact of triangulariy on plasma behaviour mostly depends on elongation value of the cross section of the tokamak torus. For example, at scan 7b, which is the case of the circle, the triangularity slightly increases the plasma growth rate and frequency; at scan 8d at κ = 2.0 increase of triangularity causes the mode change.

4.2.4 The plasma growth rate and frequency via triangularity derivative, $\nabla\delta$

It was interesting to take scans at some critical points, where modes are changing, for example at the elongation, κ = 1.5.

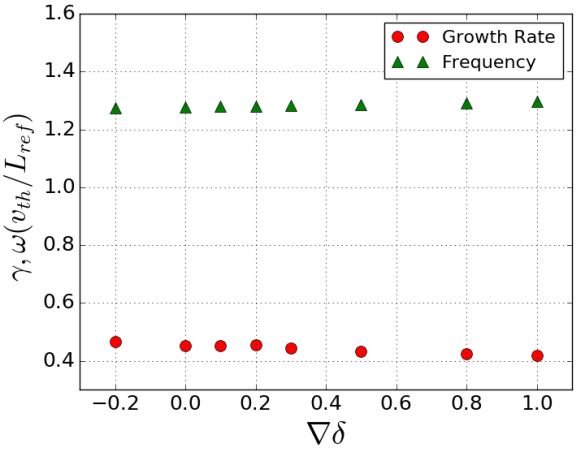

Figure 9a shows γ and ω as functions of triangularity derivative, $\nabla\delta$, at κ = 1.6 and δ = -0.1

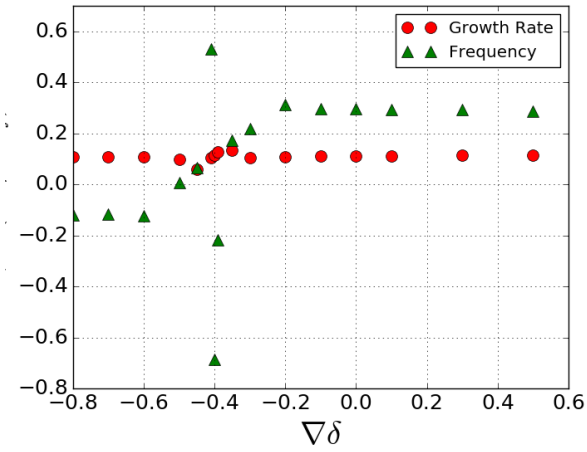

Figure 9b shows γ and ω as functions of triangularity derivative, $\nabla\delta$, at κ = 2.0 and δ = - 0.1

In general the plasma the growth rate and the frequency have a very weak dependence from triangularity derivative, $\nabla\delta$. However at these critical situation a plasma is very sensitive to triangular derivative, $\nabla\delta$, and $\nabla\delta$ can change dramatically change the plasma behaviour. For example at the scan, shown on figure 9b, a few extra plasma modes appeared because of changing of $\nabla\delta$.

4.2.5 Scans of γ and ω against major and minor radii

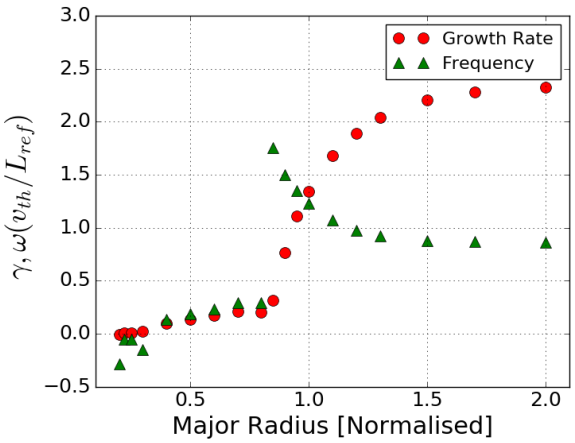

Figure 10a shows plasma growth rate and frequency via tokamak major radius.

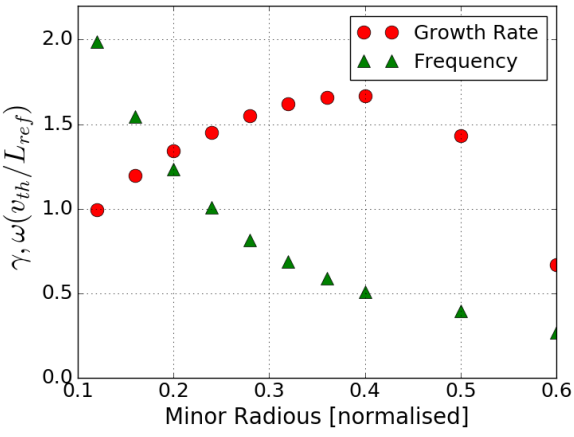

Figure 10b shows plasma growth rate and frequency via tokamak minor radius.

Although the geometry of the cross section does not depend on the tokamak minor and major radii, these parameters determine the general tokamak shape. I was exploring how these parameters

impact on the plasma behaviour. Interestingly, when the major radius becomes small and the takamak takes the spherical shape, the KBM disappears and the plasma growth rate becomes very small, and even it has negative values at some points.

5. Discussion

5.1 Discussion of the code verification and errors

Regarding verification of the code I was able to perform only convergence tests and benchmarking. It has positive results, the output parameters – the plasma growth rate and frequency converge to their limit regarding all 4 their variables at low and high β. Totally 16 convergence tests were conducted. All of them showed the convergence of the code.

The comparing of my results with already published results[2] also confirmed the correctness of the code. The curves from my and journal plots have the similar shapes, although there are some differences between the growth rates at some points. The differences can be explained by the fact that I used a linear gyrokinetic code, but the authors[2] employed a non-linear code. A linear code uses only first order of perturbations, but a non-linear code takes in account second and higher orders of perturbations, that makes the model much more accurate.

A convergence test is the only minimum criterion to be used for rigours code verification and validation, it gives some degree of confidence of the code correctness, it could represent reality and match experiment.

It is very difficult to estimate errors of output parameters, because the code at every single run at fixed parameters gives absolutely the same results. It is not the statistical distribution. However theoretically the error can not be zero. I suggest there are two types of errors may arise. The first error is numerical, which comes from the calculating techniques, which can be estimated from convergence tests, and it is less than 1%. The second error comes from the disagreement of models. For example, it may come from the model assumptions which were used to derive the gyrokinetic equation. From the difference of the results of the computer simulations, the “model” error can be roughly estimated as 10 – 20%.

5.2 Discussions of the variety of plasma modes

From the result section we can see that nearly every scan shows a few different modes: the KBM, ITG mode, ETG mode, TEM and others. Probably all these modes exist simultaneously, but the GS2 code shows only the dominant one. This is why it is very difficult to track and identify all these modes. Every mode has its own nature, driving forces and should be studied separately with appropriate physics. However, as it was mentioned in introduction, the main motivation of research is studying KBM because of its crucial role in the EPED model.

5.3 The shift of magnetic flux surfaces

Regarding to the phenomena of the shift of the magnetic flux surfaces I will try to explain why the shift happens and suggest why it reduces the plasma growth rate. The MHD equilibrium can be described by Grad-Shefranov equation[1]:

$$R^2 \nabla \left(\frac{\nabla \Psi}{R^2} \right) = -\mu_0 R^2 \frac{\partial P}{\partial \Psi} - F \frac{\partial F}{\partial \Psi} \qquad (4)$$

where F and Ψ aximetric scalar functions, F is the flux function related to the poloidal current, Ψ is the poloidal flux function, R is the tokamak radius, P is the toroidal plasma pressure.
The solution of the equation (4) will give us a formula for displacement of a magnetic flux surface of radius r[1].

$$\frac{\partial \Delta}{\partial r} = -\frac{r}{r_0} \left(\beta_p + \frac{l_i}{2} \right) \qquad (5)$$

where Δ is the Shafranov shift,
r_0 is the tokamak minor radius,
r is is the radius of magnetic flux surface,
β_p is poloidal component of magnetic confinement efficiency,
l_i is poloidal distance along the flux surface.

The physical meaning of the phenomena of the shift can be explained by magnetic field geometry of the tokamak. As the magnetic field is decreasing from the tokamak centre to outwards, a plasma placed inside the magnetic field tends to move from the area of strong magnetic field to a weaker magnetic field. The plasma tends to find the most stable position where it will reach the equilibrium between the magnetic forces and the plasma pleasure. But the plasma generates a magnetic fields itself. This will change the geometry of magnetic flux surfaces.

Because of this shift of the magnetic flux surfaces, the plasma pressure will be decreased. As the KBM is a pressure gradient driving mode I suggest this mode will be smaller because of the decreased plasma pressure. The Shafranov shift acts as a stabilising force of the plasma[11], what actually we see at figure 5b. Actually the shift suppress the KBM – at high $\beta > 4\%$ the KBM disappears. Whether the shift affects other modes or not is not clear from this simulation.

As it is mentioned before studying the KBM is important for the EPED model.[13] So the phenomena of the magnetic flux surfaces shift, which reduces the KBM, should be taken into consideration in studying of the EPED model.

5.4 Flux-surface geometry

From the data presented in the results section, the impact of the shape of the cross section on the plasma behaviour is obvious. The plasma growth rate and frequency are very sensitive to elongation but have a weak dependence on triangularity. This phenomena can be explained by features of curvature (“bad/good curvature”) of the magnetic flux surfaces, which is dependant on the elongation and triangularity. From this point the phenomena can be explained by dependence on the elongation and triangularity. The the ideal MHD equation which can be analytically derived from the ideal MHD set equations and has the expression:

$$\nabla_\perp \left(P + \frac{B^2}{2\mu_0} \right) - \frac{B^2}{\mu_0} (\boldsymbol{b} \cdot \nabla) b = 0 \quad , \qquad (6)$$

P is plasma pressure, $\boldsymbol{B}$ is the magnetic field, $\boldsymbol{k}$ is curvature of the magnetic field,

$\boldsymbol{b}=\frac{\boldsymbol{B}}{B}$ is the unit vector $\boldsymbol{B}$.

The term of curvature can be introduced:

$$\boldsymbol{k}=(\boldsymbol{b}\cdot\nabla)\boldsymbol{b}=-\frac{\boldsymbol{R}}{R_c^2} \quad (7)$$

From rearranging equation (6) the pressure gradient ∇P can be expressed as a function of the curvature, $\boldsymbol{k}$, which is determined by elongation ,κ, and triangularity, δ. But the KBM is a pressure gradient driving mode and scales with a pressure gradient, ∇P . So, the KBM growth rate depends on curvature, $\boldsymbol{k}$;or elongation, κ, and triangularity, δ.

Furthermore, figures 10a and 10b show that the plasma growth rate and frequency have a dependence on tokamak major and minor radii. Interestingly, the authors got the similar results[14],(FIG 12). The tokamak radii do not determine the torus cross section, however a tokamak magnetic flux surface can be considered as a 3 dimensional shape. The curvature of the 3 dimensional shape has a components of the tokamak major and minor radii. Similarly to dependence on elongation and triangularity, this geometry may explain why the KBM depends on the radii.

Analytically the dependence of the plasma growth rate and frequency on the curvature can be explained by an analysis of the gyrokineticks equation (3) structure. The velocity $\boldsymbol{V_0}$ in the equation (3) has some components of the curvature, κ. So, at different curvatures, κ, the velocity, $\boldsymbol{V_0}$, will have different values, which eventually will give different solution of the equation (3). From this, the plasma growth rate and frequency are dependant on the curvature or elongation, κ, and triangularity, δ.

5.5 "s-α" model

In addition the dependence of the plasma growth rate and frequency on the curvature parameters can be explained by the "s-α" model[1]. The authors [1] plotted the "s-α" space curve of the marginal ideal MHD ballooning stability at range of different triangularities, δ. Where s is the global plasma shear and α scales with β. These curves look like upside down "saddles", and divide the "α-s" space into the stable and unstable areas. From figure 11 we can see the bigger triangularity, δ , the smaller unstable area and the better ideal MHD stability is. But the KBM is a type of the ideal MHD modes, and the "s-α" model should apply for the KBM. From this point the KBM is dependant on the curvature parameters.

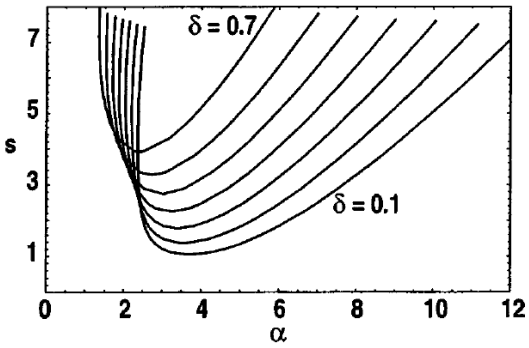

Figure 11. It is a cartoon taken from [1] shows Ballooning mode marginal stability curves for a range of triangularities, using local equilibrium parametrisation. Based upon numerical equilibrium.

6. Conclusion

My results showed that the plasma growth rate and frequency converge to some limits regarding all their main input parameters at low and high β. The code is sensitive to slight changes of input parameters. The scan of the plasma growth rate and frequency against β, has a good agreement with

the published results[2] with accuracy up to 10%. Everything this indicates on consistence and correctness of the code.

From the results it would be interesting to take Shafranov shift into consideration in the EPED model, because the shift significantly reduces the KBM. However the shift of the magnetic flux surfaces has a weak impact on other modes.

The computer simulation showed a number of plasma modes: the KBM, TEM, ITG, ETG. Each mode has its own nature and has to be studied individually. At low and high β the plasma behaves differently. At the low β the plasma behaviour is determined by a presence of the Ion Temperature Gradient (ITG) mode, but at $\beta > 1\%$ the ITG mode disappears and the the Kinetic Ballooning Mode (KBM) becomes dominant.

The ITG mode slightly decreases with the elongation, κ. To contrast to the ITG, the KBM mode is very sensitive to elongation and it is totally suppressed by elongation at $\kappa > 1.5$. However the KBM has a weak dependence on other geometry parameters as elongation derivative, $\nabla\kappa$, triangularity, δ, triangularity derivative, $\nabla\delta$.

The dependence of the KBM on the elongation can be explained by theory of “bad/good” curvatures, analysis of the gyrokinetics equation. The results have a good agreement with “s-α” model.

The tokamak minor and major radii also have influence on the plasma behaviour. At a low aspect ratio, when a tokamak takes a spherical shape, the KBM disappears and the plasma growth rate becomes incredibly low. It would be interesting to look at the tokamak pedestal at these parameters.

7. Acknowledgements

I would like to thank everyone who took part in developing the GS2 code. I am very grateful to my supervisor Dr David Dickinson for his dedication, guidance and bright ideas. Also many thanks to my co-supervisor Stephen Biggs for his help.

8. References:

[1] R. L. Miller, M. S. Chu, J. M. Greene, Y. R. Lin-Liu, and R. E. Waltz, “Noncircular, finite aspect ratio, local equilibrium model”, Physics of Plasmas 5, 973 (1998); doi: 10.1063/1.872666

[2] E. A. Belli and J. Candy, “Fully electromagnetic gyrokinetic eigenmode analysis of high-beta shaped plasmas”, Phys. Plasmas 17, 112314 (2010); doi: 10.1063/1.3495976

[3] D. Dickinson, C. M. Roach, S. Saarelma, R. Scannell, A. Kirk and H. R. Wilson, “Kinetic Instabilities that Limit in the Edge of a Tokamak Plasma: A Picture of an H-Mode Pedestal”, PRL 108, 135002 (2012), DOI: 10.1103/ PhysRevLett.108.135002

[4] N. S. Karadashev, “Cosmology and Civilizations”, March 1997, Astrophysics and Space Science, Volume 252, Issue 1–2, pp 25–40

[5] E. A. Lazarus et al, “Higher beta at higher elongation in the Dill-D tokamak”, Physics of Fluids B: Plasma Physics 3, 2220 (1991); doi: 10.1063/1.859639

[6] Lei Qi, Jaemin Kwon, T. S. Hahm, and Gahyung Jo, “Gyrokinetic simulations of electrostatic microinstabilities with bounce-averaged kinetic electrons for shaped tokamak plasmas”,
Physics of Plasmas 23, 062513 (2016); doi: 10.1063/1.4954050

[7] John A Krommes, “Nonlinear gyrokinetics: a powerful tool for the description of microturbulence in magnetized plasmas”,
Phys. Scr. T142 (2010) 014035 (13pp), doi:10.1088/0031-8949/2010/T142/014035

[8] P. B. Snyder, T. H. Osborne, K. H. Burrell, R. J. Groebner, A. W. Leonard, R. Nazikian, D. M. Orlov, O. Schmitz, M. R. Wade, and H. R. Wilson, ”The EPED pedestal model and edge localized mode-suppressed regimes: Studies of quiescent H-mode and development of a model for edge localized mode suppression via resonant magnetic perturbations”,
Physics of Plasmas 19, 056115 (2012); doi:10.1063/1.3699623

[9] S Saarelma, J Martin-Collar, D Dickinson, B F McMillan, C M Roach, “Non-local effects on pedestal kinetic ballooning mode stability”, Plasma Phys. Control. Fusion 59 (2017) 064001 (8pp), https://doi.org/10.1088/1361-6587/aa66ab

[10] D Dickinson, S Saarelma, R Scannell, A Kirk, C M Roach and H R Wilson, “Towards the construction of a model to describe the inter-ELM evolution of the pedestal on MAST”,
Plasma Phys. Control. Fusion 53 (2011) 115010 (14pp), doi:10.1088/0741-3335/53/11/115010

[11] A Merle, O Sauter and S Yu Medvedev, “Pedestal properties of H-modes with negative triangularity using the EPED-CH model”,
Plasma Phys. Control. Fusion 59 (2017) 104001 (11pp) doi.org/10.1088/1361-6587/aa7ac0

[12] C M Roach, ”Gyrokinetic and Maxwell Field Equations in GS2”, August 2011, [unpublished]

[13] M J Gerver et al, “Access to the second stability region in a high-shears low-aspect-ratio tokamaks”, The Physics of Fluids 31, 2674 (1988); doi: 10.1063/1.866545

[14] J. E. Kinsey, R. E. Waltz, and J. Candy, “The effect of plasma shaping on turbulent transport and **E** x **B** shear quenching in nonlinear gyrokinetic simulations”,
Physics of Plasmas 14, 102306 (2007); doi: 10.1063/1.2786857